JOURNAL OF OPTOELECTRONICS AND ADVANCED MATERIALS, Vol. 11, No. 12, December 2009, p. 1954 - 1958

Registration of low intensity IR radiation using modal interference in an optical fiber

I. CULEAC*, I. NISTOR, M. IOVU, A. ANDRIESH
Institute of Applied Physics of the Academy of Sciences of Moldova,
No 5 Academiei Str., MD-2028 Chisinau, Republic of Moldova

A high sensitivity fiber-optic method for registration of low intensity IR radiation is proposed. The method is based on the effect of variation of the speckle pattern in the far-field of a multimode fiber. IR radiation that falls on a lateral surface of the fiber leads to variation of the speckle image. Computer processing of the speckle image provides information on the amplitude of the perturbation that hits the fiber. An algorithm has been developed for processing of the speckle image and determining of the intensity of IR radiation. The results of computer simulation correlate sufficiently well with experimental ones.

(Received July 5, 2009; accepted November 12, 2009)

Keywords: multimode fiber, speckle pattern, modal interference, CCD, IR radiation.

1. Introduction

When injecting a coherent light beam into a multimode optical fiber the light is guided in a determined number of propagation modes. Each of these modes has a specific propagation constant, spatial field distribution and polarization. The number and the shape of confined modes are function of the index of refraction, diameter of the fiber core and the wavelength of light. At the exit end of the fiber the propagation modes interfere in the far field producing a random interference image – the speckle pattern. This pattern is highly sensitive to external perturbations and carries information on the conditions of light propagation in the fibers. The changes in the speckle pattern produced by external perturbations are determined by variation in the optical path length due to changes in the index of refraction, geometrical path and the propagation constants of each fiber mode. This effect is laid dawn on the basis of measurement techniques that employ modal interference in an optical fiber [1-3].

Seckle-based methods are widely used for registration of physical parameters [4-6]. These methods have been extensively used for industrial applications in measurement of deformation and displacement, object shape, vibrations, etc. [2,6]. Electronic speckle interferometry combined with PC processing technique offer powerful tools for registration of physical quantities and industrial control.

In the previous paper we have reported a fiber optic method for registration of low intensity infrared radiation based on the effect of interference of propagation modes in the far field of a multimode fiber [7]. In this paper we present new results and details on the method.

2. Experimental set-up

The experimental set-up is represented in Fig. 1. It consists basically of a multimode optical fiber coupled to a coherent light source, a CCD detector, and a PC for processing of the speckle image. The probing light from the coherent light source is injected into the input face of the fiber and at the output end of the fiber in the far-field the modal distribution of the probing light intensity (the speckle image) is registered. When a physical perturbation hits the fiber, the speckle pattern changes. The CCD is used for registration of the variations of the speckle pattern of the multimode fiber for subsequent PC processing.

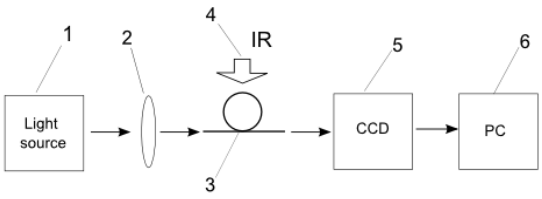

Fig. 1. Schematic representation of the method: 1 – a coherent light source; 2 – microscope objective; 3 – multimode optical fiber; 4 – IR radiation source; 5 - CCD detector; 6 – computer.

The probing light source was a HeNe Laser at 633 nm. A segment of multimode commersially available optical fiber with a parabolic index profile and the core/clading diameter 50/125 μm was used as sensing element. A common electrical heater was used as IR radiation source. Variation of the intensity of IR radiation was performed by variation of the distance between

electrical heater and optical fiber. The speckle pattern in the far field of the fiber was registered with a HDCS-1020 CMOS image sensor with the pixel size 7.4x7.4 μm and image array sizes VGA 640x480. The full frame video rate at 8-bit resolution was 30 fps.

3. Experimental results

A typical speckle pattern of the fiber used for measurements is shown in Fig. 2(a). Analyses of spatial distribution of light intensity in the speckle pattern *I(x,y)* in the far-field of the fiber provides information about the conditions of light propagation in the multimode fiber as well as on the perturbations that affect the optical fiber. The speckle image represents the result of destructive and constructive interference of propagating modes in the far field of the fiber (Fig. 2(b)). For a separate mode at the output end of fiber the magnitude of electric field $\vec{E}$ can be represented as:

$$\vec{E} = \vec{A}_0 \cos(\omega t + \varphi), \quad (1)$$

where $\vec{A}_0$ is the amplitude of electrical field, ω is the frequency of electromagnetic wave, t is the time. The phase for a separate mode φ is determined by the geometrical path length L, the wavelength λ and the effective index of refraction n ($\varphi = 2\pi n \frac{L}{\lambda}$).

The total amplitude of the electric field in any point of speckle pattern in the plane of CCD sensor can be represented as the sum of contributions of all N propagating modes of the fiber:

$$E = \sum_{k=1}^{N} |A_k| \exp(j\varphi_k), \quad (2)$$

where A_k is the amplitude of the *k-th* mode of the fiber, φ_k is the phase for the *k-th* mode at the output end of the fiber, N is the total number of modes propagating in the core of the fiber.

When two modes interfere in the point *P(x,y)* of the CCD plane the resulting intensity *I(x,y)* can be described by the relation:

$$I(x,y) = I_k(x,y) + I_{k+1}(x,y) + 2\sqrt{I_k I_{k+1}} \cos(\varphi_k - \varphi_{k+1}) \quad (3)$$

where $I_k(x,y)$ and $I_{k+1}(x,y)$ are the intensities of the *k-th* and *(k+1)-th* modes in the point *P(x,y)* of the CCD plane X_dY_d, φ_k and φ_{k+1} are respectively the phase of the *k-th* and *(k+1)-th* modes in the point *P(x,y)*. The structure of the speckle pattern depends on the coherence properties of the laser beam, refractive index profile, characteristics of the fiber and the external conditions at the core/cladding boundary.

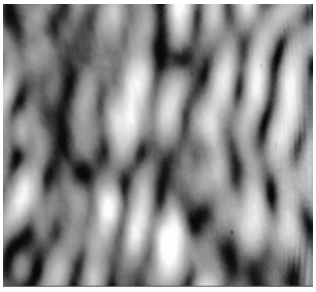

a

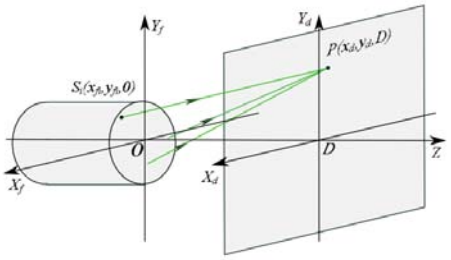

b

Fig. 2. a Illustration of the far field speckle pattern of the fiber registered by CCD sensor. (b) Schematic representation of interference of the modes in the far-field of the fiber.

The algorithm for processing of the speckle images registered by the CCD camera is based on comparison of speckle image taken at $t = 0$ and each one of the subsequent speckle images taken in the time moment t_k, where $k = 1,2,3, \ldots k_{max}$. A schematic illustration of the speckle processing algorithm is represented in the Fig. 3. The CCD camera takes an image of the speckle in the initial time t_0, and this image is stored din the buffer memory. The following speckle images are taken at the time t_k. Then the initial image I_0 is subtracted pixel-by-pixel from each of the current image I_k, and the current difference image I_k^d is obtained, where for a separate pixel belonging to I_k^d, the procedure obeys the relation:

$$I_k^d(x_i, y_j) = \left| I_k(x_i, y_j) - I_0(x_i, y_j) \right|, \quad (4)$$
$$i = 1,2,3..., r_1, \; j = 1,2,3..., r_2,$$

where $i = 1,2,3...,r_1$; $j = 1,2,3...,r_2$; and r_1 and r_2 corresponds to the CCD's *X* and *Y* resolution respectively. The next processing step represents summation of all pixels' intensity from the image I_k^d and determination of the current sum S_k for the current moment t_k as follows:

$$S_k = \sum_{i=1}^{r_1} \sum_{j=1}^{r_2} I_k^d(x_i, y_j), \quad (5)$$

The resulting value of the sum S_k is plotted on the PC screen as the output signal of the CCD detector for a specific time moment t_k (Fig. 5). The screenshot of the speckle image processing software is represented in Fig. 5. The variation of the output signal after switching on the IR radiation is represented in Fig. 6.

Application of this algorithm offers the possibility to plot on the PC screen in the real-time scale the difference of the speckles images as the output signal of the method. The magnitude S_k correlates with the amplitude of the perturbation that hits the fiber and can be calibrated to represent exactly the amplitude of the perturbation that affects the fiber.

Because we do not utilize too many routines for image processing, the rate of the procedure is sufficient high.

On the other hand, because we do not take into account the coordinate of the pixels, this algorithm does not permit to eliminate the elements that are symmetric in the speckle images. Consequently, this reduces the sensitivity and dynamic range of the method. The dependence of the output signal vs. the amplitude of the perturbation keeps linear for a sufficient wide segment of the speckle spot. Consequently, the output signal plotted on the PC screen keeps linear for a sufficient large range of the intensity of IR radiation. The sensitivity of the speckle pattern to IR radiation strongly increases when cooling down the optical fiber (Fig. 6).

4. Computer simulation

Consider interference of propagation modes in the far-field of the fiber. According to the Huygens' principle each of the point on the fiber end face $s(x_f, y_f)$ can be considered as a source of spherical waves (Fig. 3). These waves interfere constructively or destructively in the image plane of the CCD camera. The speckle pattern represents the contributions of propagating modes with a certain mutual phase difference. When external perturbation (heat, IR radiation, et.) hits the fiber the phase difference between modes will change.

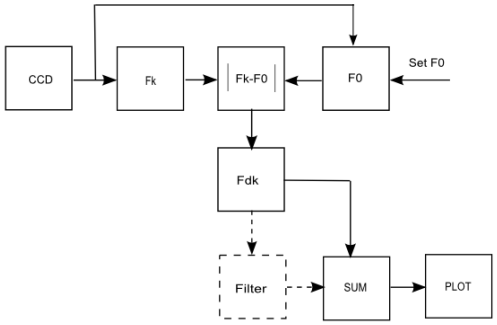

Fig. 3. Illustration of the speckle image processing algorithm

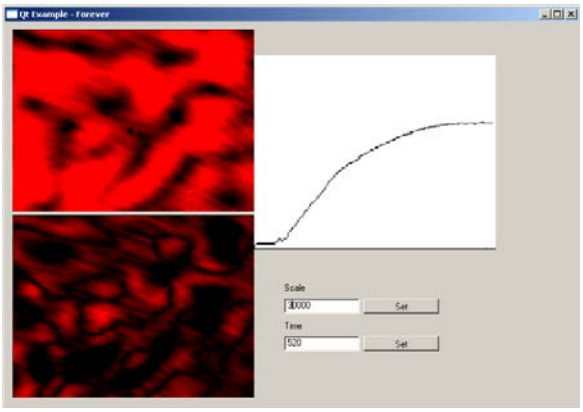

Fig. 4. The screenshot of the speckle image processing software

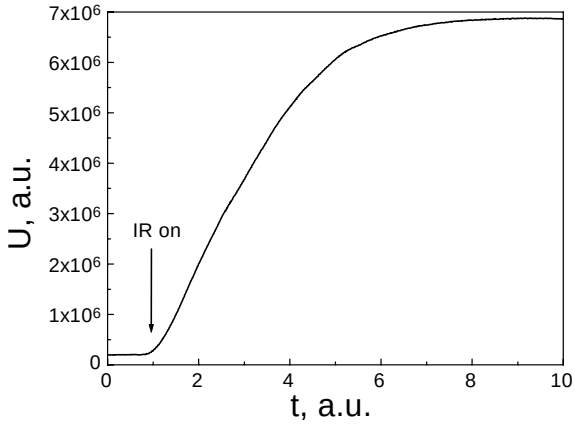

Fig. 5. Output signal characteristic after switching on the IR radiation P_{IR} = 27 μW. The light source is a HeNe laser at 633 nm.

The first speckle image I_0 is captured by CCD camera at initial time $t=0$ when launching the procedure. Then at each subsequent time moment t_k (k = 1,2,3…..k_{max}) the CCD takes the current image I_k. The difference of the two speckle images is calculated by subtracting pixel-by-pixel of two images and the value of the sum S_k is calculated with subsequent plotting on the PC monitor.

The program for computer simulation of the modal interference in the far-field of the fiber has been developed on the basis of *C++* language and run on the *Linux* platform. The PC technical profile is characterized by *AMD Sempron Processor 3000+ 1.61GHz, 1GB RAM*. The basic parameters that have been set for numerical simulation were as follows: CCD resolution, the pixel area S_p, the distance between the end face of the fiber and CCD plane D, the diameter of the core of the fiber d_{core}, the total number of propagating modes N, and the wavelength of the probing light λ.

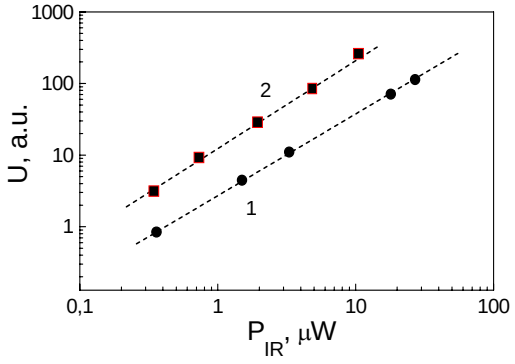

Fig. 6. The amplitude of the output signal vs. the intensity of infrared radiation. The light source is a He-Ne laser at 633nm. The temperature of the fiber: T = 290 (1); 278 (2).

Computer simulation of the output signal variation vs. the time after switching on the perturbation IR radiation has been obtained. The simulation procedure has been carried out for two cases: *a)* the ideal case without noise; *b)* the case when the far-field speckle pattern is composed of "true" signal speckle pattern, accompanied by a speckle noise. For modeling of the speckle pattern in the far-field of the fiber several points have been chosen randomly on the end face of the fiber. The speckle pattern in the far-field was obtained by coherently adding up the spherical waves originating from the random points. As few as 14 randomly selected points are enough to produce a simulated speckle pattern that correlate quite well with the signal speckle. The distance between the CCD plane and the end face of the fiber was set at 3 cm. The characteristics of the CCD in the simulation procedure have been set of the same values as ones for the real CCD in the experiment (512x512 pixels).

The results of simulation of the speckle patterns and the corresponding output signal curves are represented in Fig. 7 ad Fig. 8. The coordinates of the sources s_m on the fiber end face (x_{fm}, y_{fm}) have been generated arbitrarily to follow the relation:

$$x_{fm}^2 + y_{fm}^2 \le \rho^2, \quad m = 1,2,3,...N, \tag{6}$$

where ρ represents the diameter of the core of the optical fiber. The intensity in the point with the coordinates (x_d, z_d, y_d) that lay in the plane of the CCD sensor $X_d Y_d$, is determined by the interference of the light waves (modes) generated by the all the sources s_m with the coordinates $(x_{fm}, y_{fm}, 0)$:

$$I(x_d, y_d) = \frac{\varepsilon_0 c}{T} \int_0^T E^2(x_d, y_d, t) dt \tag{7}$$

$$E(x_d, y_d, t) = \sum_{m=1}^{N} E_m(x_d, y_d, t) = \sum_{m=1}^{N} E_{0m} \cos(2\pi \frac{d_m}{\lambda} - 2\pi \frac{t}{T} + 2\pi \frac{\varphi_m}{\lambda}) \tag{8}$$

where $T = \frac{c}{\lambda}$, and d_m is the distance between the source point $s_m(x_{fm}, y_{fm}, 0)$ and the element of the CCD matrix with the coordinates $P(x_d, z_d, D)$.

$$d_m = \sqrt{(x_d - x_{fm})^2 + (y_d - y_{fm})^2 + D^2} \tag{9}$$

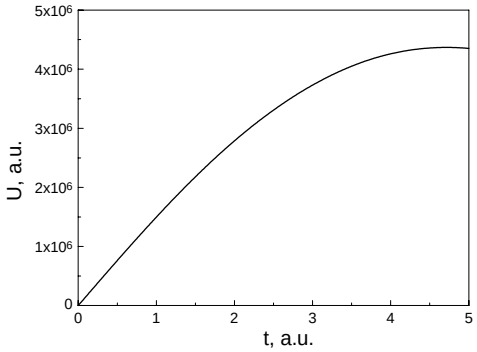

Fig. 7. Computer simulation of output signal for the case of no CCD noise.

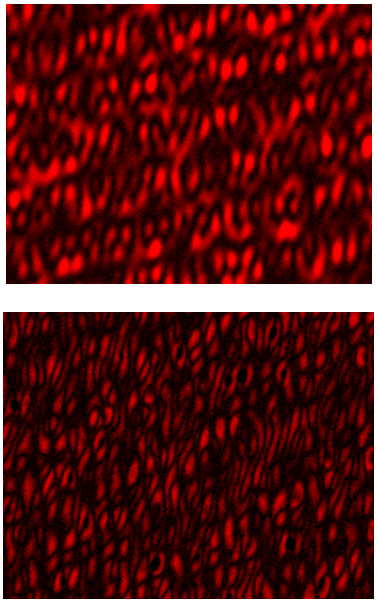

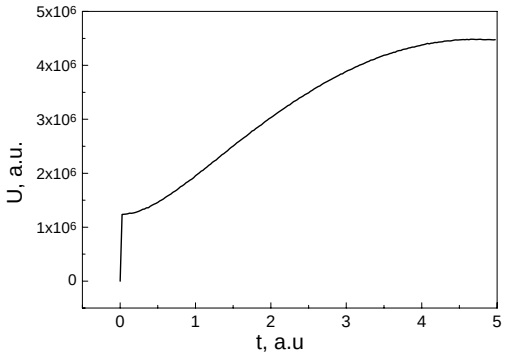

Fig. 8. Computer simulation of the speckle pattern in the far-field of the fiber and the plot of the corresponding output signal for the case of CCD noise: (a) the image of the simulated reference speckle pattern; (b) the image of the difference of the reference and the current speckle patterns ; (c) the plot of the output signal.

As far as the index of refraction *n* varies very slowly across the fiber cross-section and the optical pathway varies differently for different modes we assumed that the phase of the mode φ_m linearly changes for a small variation of the parameter τ according to the relation:

$$\varphi_m(\tau) = \varphi_{0m} + \delta_m \tau , \qquad (10)$$

where φ_{0m} has been generated arbitrarily for the domain *[0,λ]*. The linearity coefficient δ_m has been also generated arbitrarily, so that the phase variation $\Delta\varphi_m$ for each mode is different. The final intensity of the speckle image that contains a noise component the intensity of each pixel is represented as follows:

$$I(x_d, y_d)_{noise} = I(x_d, y_d) + n(x_d, y_d) \qquad (11)$$

where $n(x_d, y_d)$ represents the noise and $I(x_d, y_d)$ represents the true signal.

The results obtained from computer modeling agree quite well with the experimental result. Figure 9 for example, demonstrates a good correlation of the results obtained in the simulation procedure and experimental results. Consequently, optimizing the geometry of the fiber core/cladding structure, the glass composition, the core index profile and its temperature dependence – one can obtain an extremely high sensitivity IR sensing device.

5. Summary

A high sensitivity fiber-optic method for registration of infrared radiation has been proposed. The method is based on the effect of variation of the speckle pattern in the far-field of the fiber under the action of external perturbation. The IR radiation that falls on the multimode fiber leads to variation of the phase difference between the propagating modes that gives rise to variation of the speckle pattern in the far-filed of the fiber. Computer processing of the speckle image provides information on the amplitude of IR radiation that hits the fiber. The algorithm has been developed for processing of the speckle image and determining the intensity of IR radiation. Both experimental results as well as computer simulation data are presented. The method can be applied for measurement of temperature, IR radiation, vibrations amplitude, etc.

References

[1] J. W. Goodman, in Laser Speckle and Related Phenomena, J. C. Dainty, ed., Vol. 9 of Topics in Applied Physics (Springer-Verlag, New York, 1975).
[2] Wei An, Industrial Applications of Speckle Techniques, Doctoral Thesis, Royal Institute of Technology, Stockholm 2002.
[3] I. Balboa1, H.D. Ford, R.P. Tatam, Meas. Science and Technology, **17**, 605 (2006).
[4] G. H. Kaufmann, Optics Communications **217**, 141 (2003)
[5] L. B. Soldano, E. C. M. Pennings, IEEE J. Lightwave Technol., **13** (1995) 615.
[6] R. Jones, C. Wykes, Holographic and speckle interferometry, Cambridge University Press (1983).
[7] I. P. Culeac, I. H. Nistor, M. S. Iovu, J. Optoelectron. Adv. Mater. **11**, 380 (2009).

*Corresponding author: ion.culeac@gmail.com